



Antibacterial activity and cell viability of hyaluronan fiber with silver nanoparticles

A.M. Abdel-Mohsen^{a,b,*}, Radim Hrdina^a, Ladislav Burgert^c, Rasha M. Abdel-Rahman^a, Martina Hašová^{d,e}, Daniela Šmejkalová^d, Michal Kolář^d, M. Pekar^f, A.S. Aly^b

^a Institute of Organic Chemistry and Technology, Faculty of Chemical Technology, University of Pardubice, Studentská 95, CZ-532 10, Pardubice, Czech Republic

^b National Research Centre, Textile Research Division, El-Buhoth Street, 12311 Cairo, Egypt

^c Institute of Chemistry and Technology of Macromolecular Materials, Faculty of Chemical Technology, University of Pardubice

^d Contipro Biotech s.r.o., Dolní Dobrouč 401, 561 02, Dolní Dobrouč, Czech Republic

^e Institute of Experimental Biology, Department of Physiology and Immunology of Animals, Faculty of Science, Masaryk University, Kotlarska 2, 611 37, Brno, Czech Republic

^f Brno University of Technology, Faculty of Chemistry, Materials Research Centre, Purkyňova 118, CZ-612 00 Brno, Czech Republic

ARTICLE INFO

Article history:

Received 6 August 2012

Received in revised form 23 August 2012

Accepted 25 August 2012

Available online 12 September 2012

Keywords:

Green chemistry

Hyaluronan fiber

Silver nanoparticles

Cell viability

Antibacterial activity

Medical applications

ABSTRACT

Silver has been used since time immemorial in different chemical form to treat burns, wounds and several different infections caused by pathogenic bacteria, advancement of biological process of nanoparticles synthesis is evolving into a key area of nanotechnology. The current study deals with the green synthesis, characterization, and evaluation of the biological activity and cell viability of hyaluronan fibers with incorporated silver nanoparticles (HA-Ag NPs). Hyaluronan fiber was prepared by the dissolving of sodium hyaluronate (HA) in aqueous alkaline solution to prepare a transparent solution, which was used for the preparation of fibers by a wet-spinning technique. Consequently, hyaluronan fiber was used as capping and stabilizing agent for the preparation of fibers with silver nanoparticles. HA-Ag NPs were confirmed by transmission electron microscopy, dynamic light scattering, UV/VIS spectroscopy, scanning electron microscopy, energy-dispersive X-ray spectroscopy, thermal analysis, nuclear magnetic resonance, Fourier transform infrared spectroscopy, and X-ray photoelectron spectroscopy. HA-Ag NPs showed high antibacterial activity of against *Staphylococcus aureus* and *Escherichia coli*. Cell viability tests indicated that hyaluronan, hyaluronan fibers and hyaluronan fibers with silver nanoparticles were non-toxic on the cell growth. Two different particles size of Ag NPs (10, 40 nm) had not any toxicity till the concentration limit. These tests were performed using mouse fibroblast cell line 3T3.

Crown Copyright © 2012 Published by Elsevier Ltd. All rights reserved.

1. Introduction

Nanotechnology is the newest and one of the most promising areas of research in modern medical science. Nanoparticles exhibit new and improved properties based on size, distribution and morphology than the larger particles of the bulk materials from which the particles are made (Jae & Beom, 2009). The surface to volume ratio of the nanoparticles is inversely proportional with to their size. The biological effectiveness of nanoparticles can increase proportionally with an increase in the specific surface area due to the increase in their surface energy and catalytic reactivity (Singh, Jain, Upadhyay, Khandelwal, & Verma, 2010). Although there are many routes available for the synthesis of nanoparticles, there is

an increasing need to develop high-yield, low cost, non-toxic and environmentally friendly procedures (Emilio et al., 2012; Panacek et al., 2009; Robert & Zboril, 2011). Silver has long been recognized as an effective antimicrobial agent that exhibit low toxicity in human and has diverse in vitro and in vivo applications (Farooqui, Chauhan, Krishnamoorthy, & Shaik, 2010). Currently, silver-based optical dressing and widely used to treat infections in open wound and chronic ulcers. These dressing also protect the host materials from oxidation and discoloration (Upendra, Preeti, & Anchal, 2009).

Wound dressings are usually used to encourage the various stages of wound healing and create better healing conditions. They often cover the wound surface to accelerate its healing. A desirable wound dressing should (a) create and keep the moist environment, (b) protect the wound from secondary infections, (c) absorb the wound fluids and exudates, (d) reduce the wound surface necrosis, (e) prevent the wound desiccation, (f) stimulate the growth factors and also be (g) elastic, non-antigenic and biocompatible (Lin, Chen, & Run, 2001; Purna & Babu, 2000). Based on the types of wounds and modes of healings, numerous materials are developed for use

* Corresponding author at: Institute of Organic Chemistry and Technology, Faculty of Chemical Technology, University of Pardubice, Studentská 95, CZ-532 10, Pardubice, Czech Republic. Tel.: +420 773063837; fax: +420 466 038 004.

E-mail address: abdo.mohsennc@yahoo.co (A.M. Abdel-Mohsen).

as wound dressing. These materials include synthetic polymers like polyurethane, poly (lactic acids), silicon rubber and natural polymers such as alginates, chitosan, gelatin and collagen (Dagalakis, Flink, Stasikelis, Burke, & Yannas, 1980).

With the increasing awareness of environmental protection, people are inclined to focus on the green chemistry. For this purpose, the natural compounds like D-glucose (Raveendran, Fu, & Wallen, 2003) and chitosan (Abdel-Mohsen, Abdel-Rahman, et al., 2012; Abdel-Mohsen, Aly, Hrdina, & El-Aref, 2012; Dash, Chiellini, Ottenbrite, & Chiellini, 2011; Wan, Sun, Li, & Li, 2009) was used to stabilize the Ag nanoparticles with other reducing agents. In addition, the soluble starch has been used as both the reducing and stabilizing agents to synthesize the Ag nanospheres via a one-pot green method (Vigneshwaran, Nachane, Balasubramanya, & Varadarajan, 2006).

Green synthesis of Ag-NPs involve three main steps, which must be evaluated based on green chemistry perspectives, including selection of solvent medium, reducing agent, and nontoxic substance for Ag NPs stability (Raveendran, Fu, & Wallen, 2006). Three main steps in the preparation of nanoparticles that should be evaluated from a green chemistry perspective are the choice of the solvent medium used for the synthesis, the choice of an environmentally benign reducing agent, and the choice of a nontoxic material for the stabilization of the nanoparticles. Most of the synthetic methods reported to date rely heavily on organic solvents. This is mainly due to the hydrophobicity of the capping agents used. There have been approaches reported (Templeton, Chen, Cross, & Murray, 1999) for the synthesis of water-soluble metal nanoparticles. However, to date a unified green chemistry approach to the overall process of nanoparticle production has not been reported.

Hyaluronan (HA) is a high molecular weight glycosaminoglycan in extracellular matrix (ECM) and plays a vital role in maintaining tissue integrity, as well as in facilitating adhesion and differentiation of cells during inflammation, wound repair, and embryonic development. HA has been implicated in the formation of vessels for years (Slevin et al., 2007; Slevin, Kumar, & Gaffney, 2002; West, Hampson, Arnold, & Kumar, 1985). In animal models, topically applied HA accelerated dermal wound healing and decreased fibrosis and scar formation in rats and hamsters (Lees, Fan, & West, 1995; Proctor et al., 2006; Rajapaksa, Cowin, Adams, & Wormald, 2005; Schimizzi et al., 2006; Takahashi et al., 2005). HA is also used as a carrier for other wound healing agents and in cosmetic formulations (Price, Berry, & Navsaria, 2007; Tezel & Fredrickson, 2008). These biological effects of HA are complex and one mechanism, the regulation of angiogenesis, has been reported to be involved, which depends on HA concentration and molecular size (David-Raoudi et al., 2008). It is generally accepted that high molecular weight HA (HMW-HA) inhibits endothelial cell (EC) proliferation, a phenomena supporting by the findings that avascular regions are rich in HMW-HA and that expression of this form of HA in normally vascular areas results in decreased vascularity (Marsano et al., 2007; Smith et al., 2008). In contrast, low molecular weight HA or oligosaccharides of hyaluronan (o-HA) stimulates EC proliferation, induces in vitro endothelial tube formation, and stimulates neo-vascularization in chick chorioallantoic membranes and collagen production by endothelial cells (Rooney, Wang, Kumar, & Kumar, 1993; Slevin et al., 2002; West et al., 1985).

In the present approach, methanol, ethanol, and propan-2-ol were utilized as the environmentally benign solvent and reducing agent throughout the preparation. The second concern in a green nanoparticle preparation method is the choice of the reducing agent. The majority of methods reported to date use reducing agents for preparation of Ag-NPs. The use of a strong reducing agent, such as NaBH_4 , results in tiny particles that are well-dispersed (Ji, Chen, Wai, & Fulton, 1999; Shah, Holmes, Doty, Johnston, & Korgel, 2000). Nowadays, a succession of chemical reductants used

for synthesis of noble metal nanoparticles which contain NaBH_4 (Shameli, Ahmad, & Yunus, 2010; Shen, Shi, & Li, 2010), ethylene glycol (Wang, Ren, & Deng, 2000), citrate (Pathak, Greci, & Kwong, 2000), or ascorbic acid (Lim, Jiang, & Yu, 2010). The final and perhaps most important issue in the preparation of nanoparticles is the choice of the capping material used to protect or passivity the nanoparticle surface. There are several issues that should guide the choice of the capping agent, and these vary significantly from the required size ranges and morphologies of the nanoparticles to the targeted application. In the presented preparation method, a hyaluronan fiber (a hyaluronan molecule) serves as the protecting and stabilizing agent.

Thus, in this work the hyaluronan fiber was prepared and used it as the capping and stabilizing agent to prepare the Ag nanoparticles, where the effect of solvents medium on the particle size of silver nanoparticles were studied. HA-Ag NPs were confirmed by TEM, DLS, UV/VIS spectroscopy, SEM, EDX, TGA, DTG, DSC NMR, FTIR, and XPS. HA-Ag NPs showed high antibacterial activity against *Staphylococcus aureus* and *Escherichia coli*. Cell viability tests indicated that hyaluronan, hyaluronan fibers and hyaluronan fibers with silver nanoparticles were non-toxic on the cell growth. Two different particles size of Ag NPs (10, 40 nm) had not any toxicity. These tests were performed using mouse fibroblast cell line 3T3.

2. Experimental

2.1. Materials

Sodium hyaluronate high molecular weight (1.75 MDa, determined by SEC-MAALS) was purchased from CPN Ltd., Dolní Dobrouč, Czech Republic, sodium hydroxide, formic acid, acetic acid, silver nitrate, ethanol, propan-2-ol, and methanol were obtained from Sigma–Aldrich, Germany. Demineralized water was used for all experiments.

2.2. Methods

2.2.1. Preparation of hyaluronan fibers

Hyaluronan fiber was successfully prepared via previous work (Abdel-Mohsen, Hrdina, et al., 2012; Burgert, Hrdina, Masek, & Velebný, 2012). Briefly, a sodium hyaluronate (1.75 MDa, 6 g) was dissolved under stirring in 94 g of water with the addition of NaOH (0.64 g) to obtain homogenous, well-flowing viscous solution suitable for spinning. This solution was pressed (wet-spinning technique) through a nozzle with the diameter of 0.4 mm to the coagulation bath having the composition: 600 ml of methanol and 400 ml of acetic acid (98%). The prepared fibers were left in the coagulation bath for 15 h, then washed with absolute methanol and dried.

2.2.2. Preparation of silver nanoparticles incorporated in hyaluronic fibers

Silver nanoparticles were prepared by means of a simple chemical reduction of silver nitrate by hyaluronic fibers (Abdel-Mohsen, Hrdina, et al., 2012). A certain weight of the so-prepared (HA fiber) was dispersed in a certain volume of methanol, ethanol and propan-2-ol using a heating magnetic stirrer. After dispersion of HA in different dispersing agents, the pH of the solution was adjusted within the range (4–11.5), followed by the raising of temperature (20–80 °C). A certain amount of silver nitrate solution was then added drop-wise. The reaction mixture was kept under continuous stirring for different time (15–180 min). Short time after the addition of silver nitrate, the HA fiber acquires a clear yellow color indicating the formation of silver nanoparticles. The progression of the reaction was controlled by UV/Vis absorption; aliquots from

the reaction bulky were withdrawn at given time intervals and evaluated.

2.3. Characterization of silver nanoparticles incorporated hyaluronic fibers

2.3.1. Scanning electron microscopy (SEM)

The images of samples were done at the electron-scanning microscope at the CPN Ltd., Tuscan VEGA II LSU electron microscope (Tuscan USA Inc.) under the following conditions: high voltage 5 kV, working distance 4.4 mm, display mode secondary electrons, high vacuum room temperature. SC7620 Mini Sputter Coater (Quorum Technologies, UK) applied 15 nm layers of gold particles on the sample. The samples were dusted for 120 s with the current of 18 mA. The pictures were made at these conditions: voltage 2.44–10 kV, detector-SE, the magnification 300–20,000 times, vacuum high, the distance between sample and objective: 4–5 mm.

2.3.2. UV-visible spectroscopy (UV-vis)

Measurements were carried out on UV-visible spectrophotometer (UV-160A, Shimadzu, Japan) using quartz cuvettes with an optical path of 1 cm. The concentration of the measured solutions was kept at 0.59 mg/ml.

2.3.3. Transmission electron microscopy (TEM)

TEM images were observed on a JEOL JEM-2010 (HT) electron microscope, using an accelerating voltage of 200 kV. The samples were dissolved in deionized water or aqueous alkaline solution with concentrations of 0.5 mg/ml, and a drop was placed on Cu grids pre-coated with carbon films.

2.3.3.1. Dynamic light scattering (DLS). DLS measurements were performed with a Malvern Zetasizer Nano ZS. The samples were prepared by dissolving 4–10 cm of the material in 1.5 ml of 0.67 M NaOH. All samples were filtered using a 0.45 μm nylon syringe filter (VWR) directly into a polyacrylic cell.

2.3.4. Cell viability assay

3000 NIH (3T3) cells/well were seeded to wells of 96-well test plates. The cells were cultured for 24 h before treated with the tested solutions. Cell viability was measured 0, 24, 48, 72 h after treatment using the 3-(4,5-dimethylthiazol-2-yl)-2,5-diphenyl tetrazolium bromide (MTT) assay. In the assay, MTT is reduced by viable cells to a colored formazan salt, which is later released from the cells and determined spectrophotometrically. MTT assay was described previously (Vistejnova et al., 2009). Cell viability was measured 0, 24, 48, 72 h after treatment using the 3-(4,5-dimethylthiazol-2-yl)-2,5-diphenyl tetrazolium bromide (MTT, Sigma–Aldrich) assay. MTT assay was described previously (Vistejnova et al., 2009). MTT stock solution was added to the cell culture medium and plates were incubated at 37 °C for 2.5 h. The supernatant was discarded and cells were lysed in lysis solution for 30 min on a shaker. The optical density was measured in 96-well plate in triplicate by a Versamax microplate reader (Molecular devices, CA, USA) at a wavelength of 570 nm.

2.3.4.1. Cell culture. Mouse fibroblast cell line (NIH 3T3) (Sigma–Aldrich) was cultured till 20th passage. Cells of 10th–20th passage were used in the following experiments. NIH 3T3 were grown in DMEM medium supplemented with 10% FBS, glutamine (0.3 mg/ml), penicillin (100 U/ml) (Sigma–Aldrich) and streptomycin (0.1 mg/ml) (Sigma–Aldrich) in 7.5% CO₂ at 37 °C in culture flask as recommended by the supplier.

2.3.4.2. Preparation of solutions. Solutions of derivatives were prepared using cell cultivation medium to obtain a final concentration

of 1000 $\mu\text{g/ml}$, and filtrated (thorough sterile filtration device (0.22 μm) to produce sterile solutions to be tested for cell viability. The tested solution was added to each well so that the final concentration of the tested solution in the well was 1–1000 $\mu\text{g/ml}$ using as diluent medium.

2.3.4.3. Statistical analysis. All experiments were carried out at least in independent repeats. The Student test for two samples was applied on the data, $p \leq 0.05$.

2.4. Antibacterial assay

2.4.1. Culture media used

Muller–Hinton agar medium(g/l)	
Beef extract powder	3
Casein hydrolase	17.5
Starch	1.5
Agar	17.0

2.4.2. Preparation of agar

Muller–Hinton agar (38 g) was suspended in one liter of distilled water, heated to dissolve the medium completely then sterilized by autoclaving at 121 °C for 15 min (Difco et al., 1969).

2.4.3. Test organisms

- The Gram positive bacteria: *S. aureus*.
- The Gram negative bacteria: *E. coli*.

2.4.4. Antibacterial test

The antibacterial activity of hyaluronan fibers with silver nanoparticles were evaluated by the disc diffusion method using sterile Whatman-No. 5 filter paper discs (11 mm diameter). Each compound (100 μg) was dissolved in deionized water (1 ml). Filter paper discs (11 mm) were loaded with certain amount of the tested material (50 μl) then left with care under hot air to complete dryness. Test plate were prepared by pouring 10 ml Muller–Hinton agar medium seeded with the test organism. The discs were deposited on the surface of agar plates along with control disc, which loaded only with used solvent (Bauer, Kirby, Sherris, & Truck, 1966). The discs were incubated at 5 °C for 1 h to permit good diffusion. All the plates were then incubated for 24 h at 37 °C. The zones of inhibition were measured.

2.5. Thermal analysis measurements

Samples were studied with regard to the kinetics of thermal decomposition, using different heating rate thermogravimetry (TG, Netzsch 209F3 instrument, Al₂O₃ crucible) and under heating rates of 5 (with data collecting rate of 40 points/K) and 10 5 °C min^{−1} (with data collecting rate of 60 points/K). The test temperature range for TG was 50–400 °C with the sample mass of about 1.35–1.45 mg under 30 ml min^{−1} dynamic nitrogen atmosphere. Samples were further analyzed by the technique of differential scanning calorimetry (DSC, Netzsch 200F3 instrument, aluminum pan with a pin hole cover), which was performed in the dynamic nitrogen atmosphere with a pressure of 0.1 MPa. The sample mass for DSC was about 0.9 mg with a heating rate of 5 °C min^{−1} and temperature range of 30–350 °C.

2.6. X-ray photoelectron spectroscopy (XPS)

XPS measurements were carried out on a VG MicroTech ESCA 3000 instrument at a pressure $>1 \times 10^{-9}$ Torr. The general scan and Au 4f, Ag 3d, C 1s, S 2p, and N 2p core-level spectra were

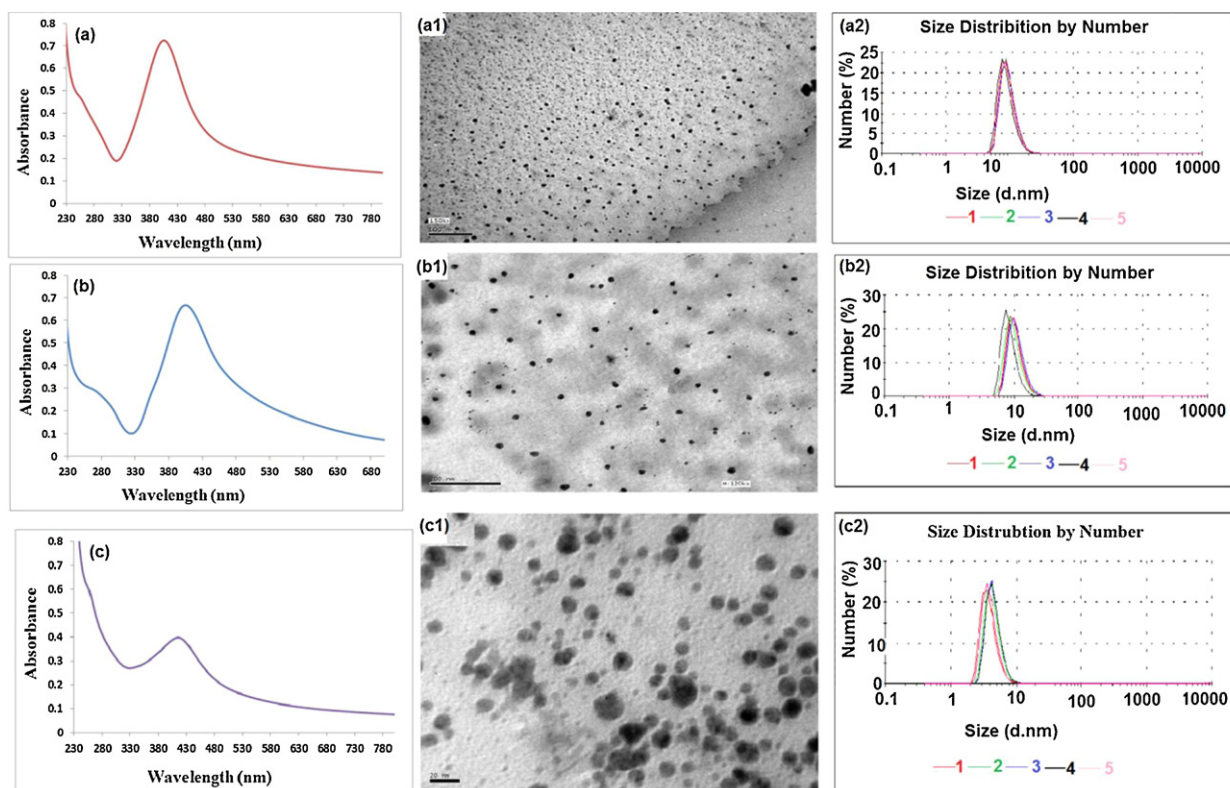


Fig. 1. Effect of different solvents in particle size of silver nanoparticles. (a, a1, a2) UV/Vis spectra, TEM, and DLS of HA-Ag NPs by using methanol; (b, b1, b2) UV/Vis spectra, TEM, and DLS of HA-Ag NPs by using propan-2-ol. Experimental conditions: hyaluronan fiber (0.1 g, 0.26 mM); temperature 60 °C; reaction time 60 min; pH 11.5; AgNO₃ concentration 10 mM (700 μ l).

recorded with un-monochromatized MgK α radiation (photon energy 1253.6 eV) at a pass energy of 50 eV and an electron take-off angle (angle between electron emission direction and surface plane) of 60°. The overall resolution was \sim 1 eV for the XPS measurements. The core-level binding energies (BE) were aligned by taking the adventitious carbon binding energy as 285 eV.

2.7. Fourier transforms infrared spectroscopy (FTIR)

FTIR spectroscopy was performed on a Shimadzu spectrometer. Samples were analysed as KBr discs; approximately 30 mg of the sample and 60 mg of KBr were blended and triturated in agate mortar. The mixture was then compacted using an IR hydraulic press at a pressure 90 kN for 1 min. The scans were conducted within 4000–600 cm⁻¹ at a resolution of 4 cm⁻¹.

2.8. Nuclear magnetic resonance spectroscopy (NMR)

NMR spectra were measured on BRUKER AV 500 MHz Ultra-shield plus with the probe BBOF plus. Samples (5–10 mg) were dissolved in D₂O.

3. Results and discussion

3.1. Preparation of hyaluronan fibers with silver nanoparticles

Hyaluronan fibers were prepared by wet-spinning technique described in previous works (Abdel-Mohsen, Hrdina, et al., 2012; Burgert et al., 2012). Hyaluronic acid was dissolved in slightly alkali water solution of sodium hydroxide, after dissolution completely of hyaluronic acid to obtain transparent solution (5.96 mass % of HA). The solution of hyaluronic acid solution was used

for wet spinning, where the nozzle had the diameter 0.4 mm. As the coagulation bath, the mixture of 600 ml of methanol and 400 ml of acetic acid (98%) was used; homogenous fibers were obtained. The prepared fibers were left in the coagulation bath for 15 h, then washed with absolute methanol and dried.

Hyaluronan fibers played a dual role: as a capping (template) agent for silver ions and as a stabilizing agent during/after the formation of silver nanoparticles. Factors affecting the reduction efficiency and stability as well as the shape and the size of the formed silver nanoparticles along with mechanisms involved are described in previous work (Abdel-Mohsen, Hrdina, et al., 2012).

Many workers (Antonio & Andre, 2010; Kim, 2007a, 2007b; Luis & Isabel, 1996) used different solvent such as methanol, ethanol, DMF in the preparation of silver nanoparticles. Since the alcohols have some reductive power, the effect of different solvent medium on the preparation of silver nanoparticles inside of HA-fiber was studied in this work. The UV–vis spectra, transmission electron microscope (TEM) and dynamic light scattering (DLS) of hyaluronan fibers with silver nanoparticles (HA-Ag NPs) prepared in different solvent medium are presented in Fig. 1. It can be concluded that the change of the solvent medium (methanol, ethanol, propan-2-ol) is changing the particle growth forming particle sizes from 10 \pm 0.5 (methanol) to 9.7 \pm 0.5 nm (ethanol) and 3.5 \pm 0.5 nm (propan-2-ol).

3.2. SEM of hyaluronan fiber with silver nanoparticles in different solvent medium

Fig. 2 shows the scanning electron microscopy of hyaluronan fibers with silver nanoparticles prepared in different solvent systems. It can be seen, that the surface

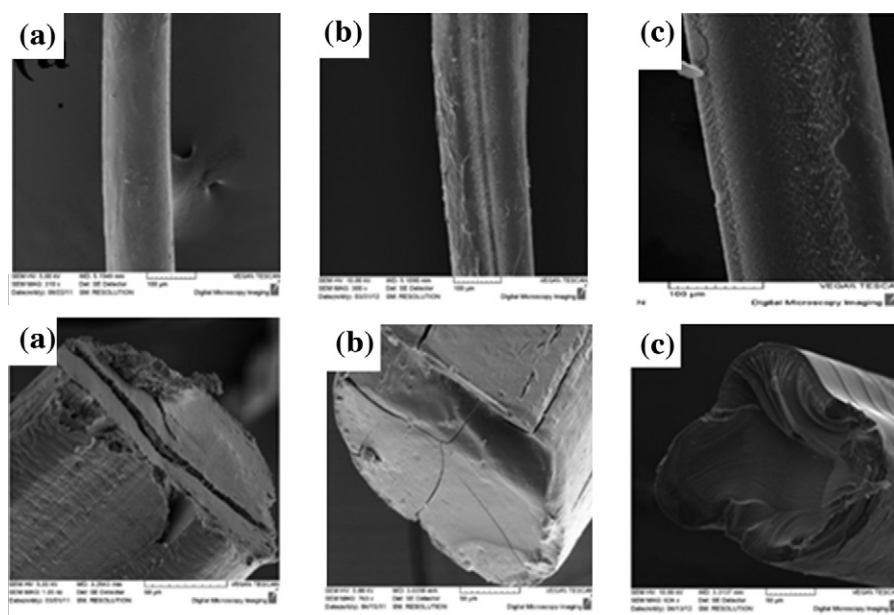


Fig. 2. SEM of hyaluronan fiber with silver nanoparticles in different solvent medium. (a) Methanol, (b) ethanol, (c) propan-2-ol. Experimental conditions: hyaluronan fiber (0.1 g, 0.26 mM); temperature 60 °C; reaction time 60 min; pH 11.5; AgNO₃ concentration 10 mM (700 μ l).

morphology and cross-section of HA-Ag NPs is more smooth, clear and homogenous in the case of methanol used as the solvent than the fibers prepared by using ethanol and propan-2-ol respectively.

3.3. FTIR of hyaluronan fiber with silver nanoparticles

Fig. 3 shows the FTIR spectra of hyaluronan, hyaluronan fibers, and hyaluronan fibers with silver nanoparticles prepared in different solvent media (methanol, ethanol, and propan-2-ol). No new peaks occurred in the FTIR spectra within the preparation of silver nanoparticles in different medium solvents.

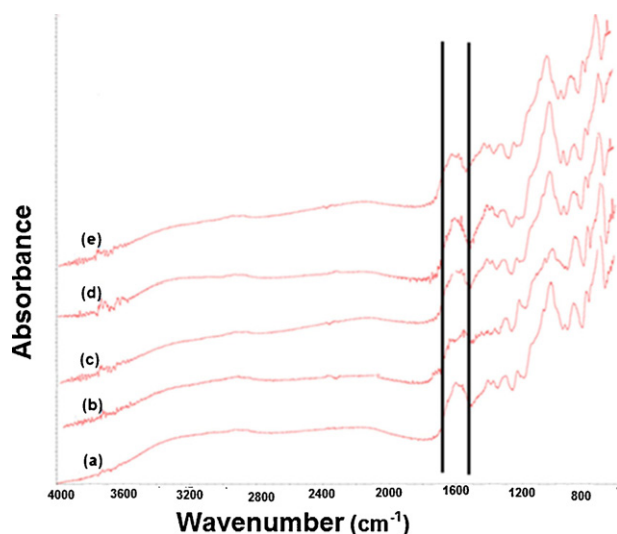


Fig. 3. FTIR spectra of hyaluronan fiber with silver nanoparticles prepared in different solvent system. (a) Pure hyaluronan; (b) hyaluronan fiber; (c) HA-Ag NPs in methanol; (d) HA-Ag NPs in ethanol; (e) HA-Ag NPs in propan-2-ol. Experimental conditions: hyaluronan fiber (0.1 g, 0.26 mM); temperature 60 °C; reaction time 60 min; pH 11.5; AgNO₃ concentration 10 mM (700 μ l); particle size 10 nm.

3.4. NMR spectra of hyaluronan, hyaluronan fiber with silver nanoparticles

Fig. 4 shows the ¹³C NMR of hyaluronan fiber (Fig. 4a) and hyaluronan fiber with silver nanoparticles (Fig. 4b). Both spectra show typical resonances of hyaluronic acid: C=O resonances at around 170 ppm, anomeric C at 106–103 ppm, skeletal signals from 85 to 54 ppm and CH₃ signal at 22 ppm. Additional signal at 23.7 ppm can be attributed to the methyl resonance from residual solvent. Small chemical shifts of C=O signals and skeletal resonances at 74 ppm can be explained by the fact that hyaluronan fiber was analyzed in its sodium form, while hyaluronan fiber with silver nanoparticles was analyzed in its acid form. Comparing the signals in Fig. 8 it is evident that during the preparation of silver nanoparticles with hyaluronan fiber there was no significant oxidation of the original hyaluronan. This result suggests that the reduction agent of Ag⁺ is in the fact used alcohol. After the reaction with silver nanoparticles, hyaluronan fiber still keeps its original resonances with comparable relative intensities. Therefore, hyaluronan fiber mainly served as stabilizing and capping agent and the chemical

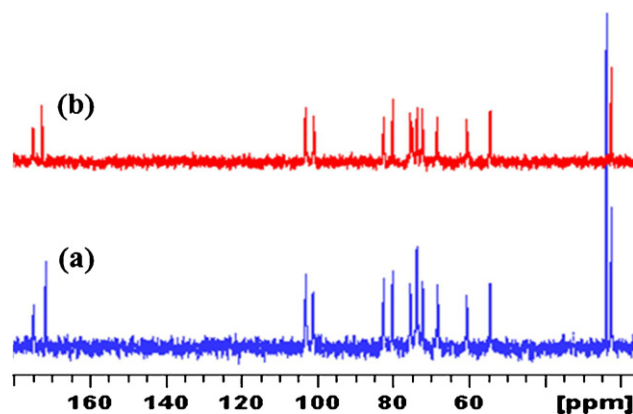


Fig. 4. ¹³C NMR spectra of hyaluronan fiber with silver nanoparticles. Experimental conditions: hyaluronan fiber (0.1 g, 0.26 mM); temperature 60 °C; reaction time 60 min; pH 11.5; AgNO₃ concentration 10 mM (700 μ l); particle size 10 nm.

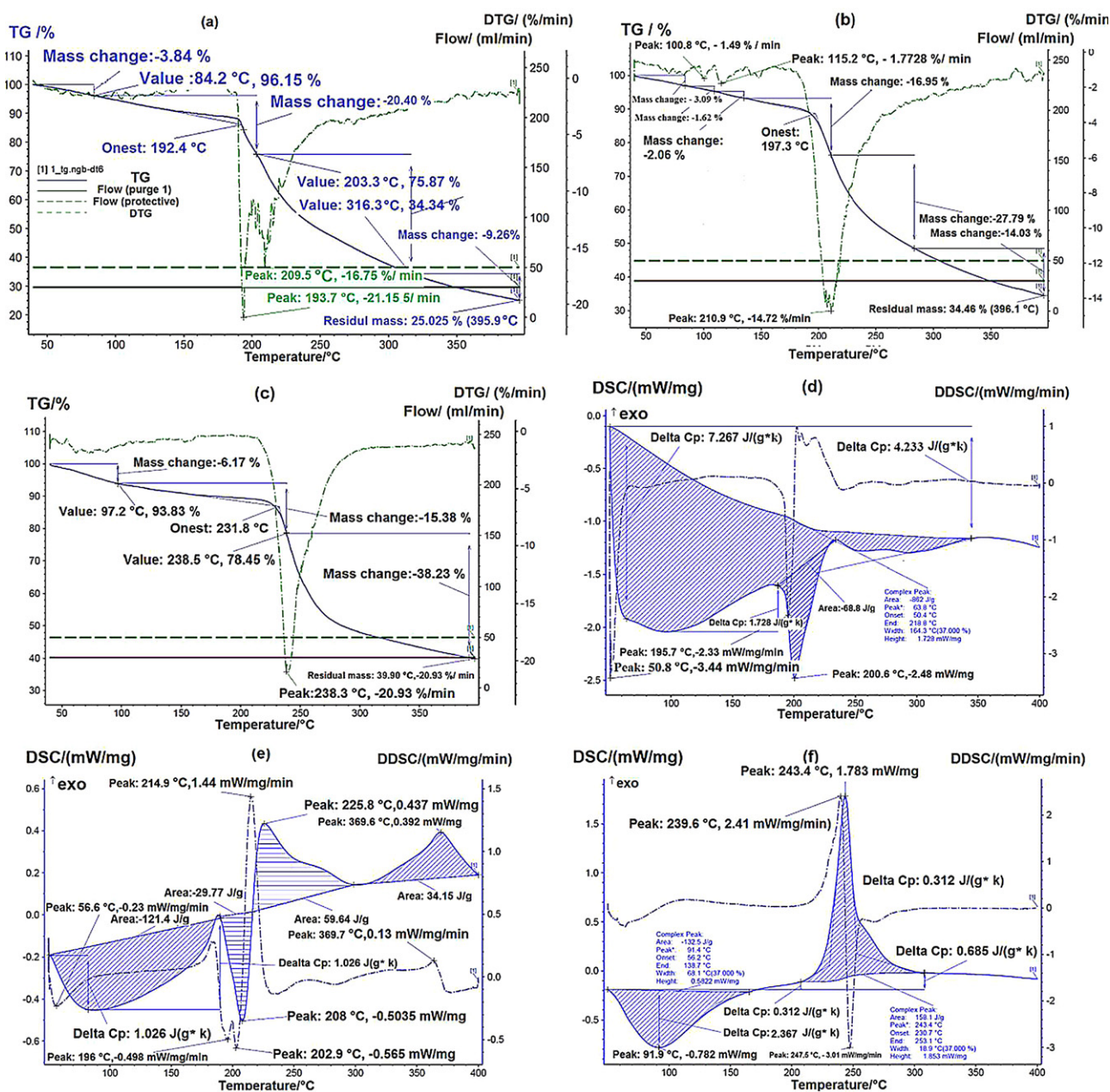


Fig. 5. TGA, DTG and DSC of pure hyaluronan, hyaluronan fiber, hyaluronan fiber with silver nanoparticles. (a) TGA, DTG of hyaluronan; (b) TGA, DTG of hyaluronan fiber; (c) TGA, DTG of hyaluronan fiber with silver nanoparticles; (d) DSC of hyaluronan; (e) DSC of hyaluronan fiber; (f) DSC of hyaluronan fiber with silver nanoparticles. Experimental conditions: hyaluronan fiber (0.1 g, 0.26 mM); temperature 60 °C; reaction time 60 min; pH 11.5; AgNO₃ concentration 10 mM (700 μ l); particle size 10 nm.

reduction of silver nitrate to silver nanoparticles was caused by used solvent system (methanol, ethanol, and propan-2-ol).

3.5. Thermogravimetric (TGA), differential thermo-gravimetric (DTG) and differential scanning calorimetric (DSC) analysis

Fig. 5 shows the thermal gravimetric analysis (TGA), differential thermal analysis (DTG), and differential scanning calorimetric (DSC) of starting hyaluronan, pure hyaluronan fibers, and hyaluronan fibers with silver nanoparticles. Fig. 5a–c shows the TGA, DTG of starting hyaluronan, hyaluronan fibers, and hyaluronan fibers with silver nanoparticles respectively. All three samples show different behavior. The first mass loss is of the same relative amount (about 10%) but is “finished” at different temperatures: $t_{\text{hyaluronan fiber}} < t_{\text{hyaluronan}} < t_{\text{hyaluronan fiber with silver nanoparticles}}$. It can

be attributed to the loss (evaporation) of water or other volatile components. The end of the first mass loss is probably not due to complete evaporation but due to the onset of sample degradation – the order of temperatures can be considered as an indicator of samples stability which is increasing in the order hyaluronan fiber < hyaluronan < hyaluronan fiber with silver nanoparticles. Thus making fibers from hyaluronan their decreases its stability, fibers containing silver are somewhat more stable than fibers from pure hyaluronan and hyaluronan fiber.

The data of DTG record of hyaluronan fiber (Fig. 5a) shows two peaks indicating two degradation processes; the existence of the second peak is suggested also for hyaluronan (Fig. 5c). This could indicate that making fibers from hyaluronan retains its degradation pattern but shifts it to lower temperatures. Silver nanoparticles in fibers seem to suppress the first degradation step (while retaining

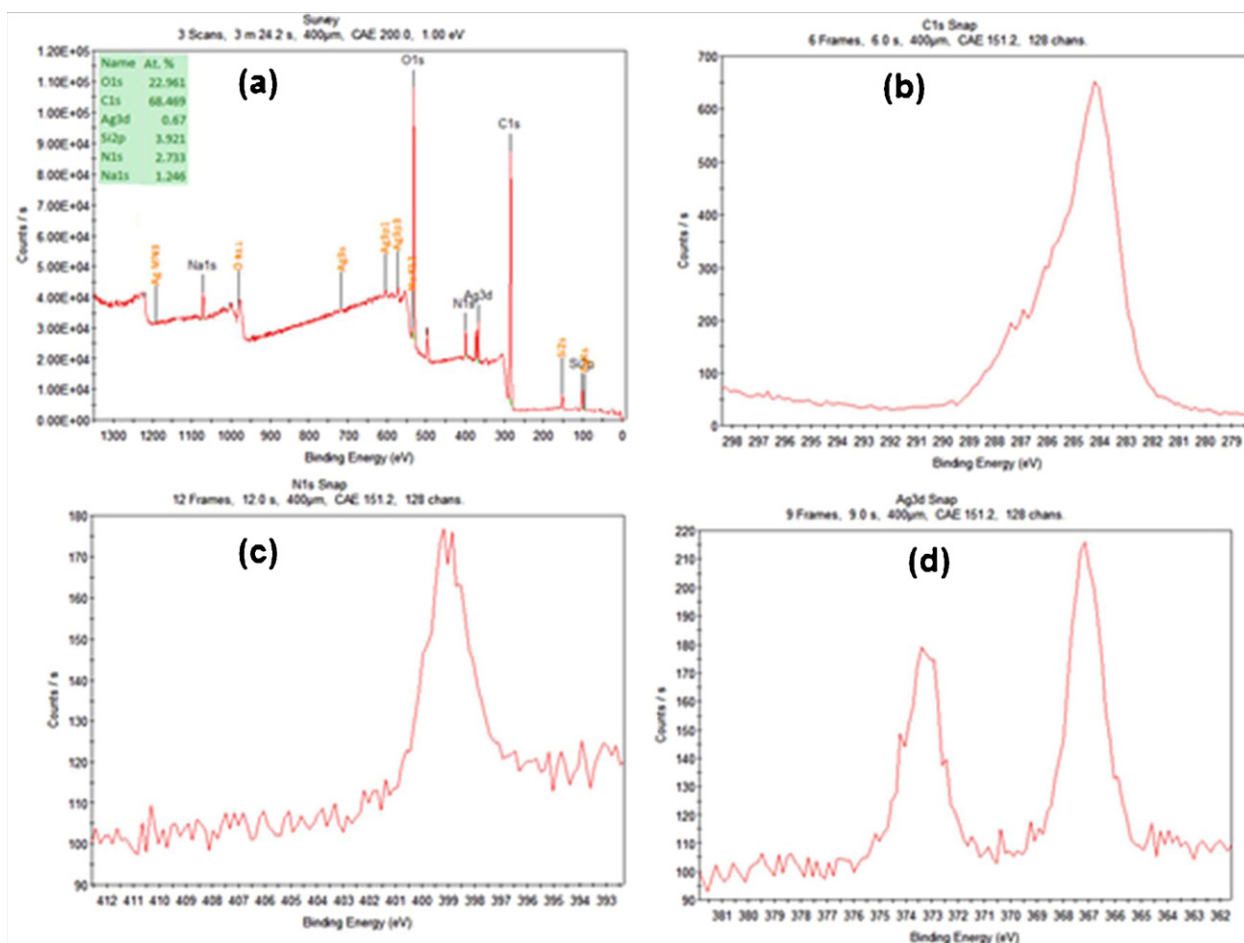


Fig. 6. XPS spectra of hyaluronan fiber-encapsulated silver nanoparticles. (a) XPS survey spectrum; (b) binding energy spectrum for C 1s; (c) binding energy spectrum for N 1s; (d) binding energy spectrum for Ag 3d. Experimental conditions: hyaluronan fiber (0.1 g, 0.26 mM); temperature 60 °C; reaction time 60 min; pH 11.5; AgNO₃ concentration 10 mM (700 μl); particle size 10 nm.

the shift of the second step) – functional groups degraded in this step should be blocked by silver. This interpretation is based on the coincidence of the second DTG peak of hyaluronan fiber (Fig. 5a) and DTG peak of sample hyaluronan fiber with silver nanoparticles (Fig. 5c).

Residual masses were different for different three samples: for hyaluronan fiber, hyaluronan fiber incorporated with silver nanoparticles, and pure hyaluronan were 25.05%, 34.45%, and 39.9% respectively, but the degradation was not completed at the highest temperature used to (400 °C). It could be attributed to the complex process including dehydration of disaccharide units in hyaluronan chains. Fig. 5d–f shows the differential scanning calorimetric (DSC) of hyaluronan, pure hyaluronan fibers, and hyaluronan fibers with silver nanoparticles. Up to about 180 °C the behavior of all samples is similar – broad endothermic peak, not very distinct for pure hyaluronan fibers, and hyaluronan fibers with silver nanoparticles (Fig. 5e and f) respectively, attributable to water and volatiles evaporation. This is in accord with TG records. Above this temperature the behavior of pure hyaluronan fibers and hyaluronan fibers with silver nanoparticles (Fig. 5e and f) is similar and significantly different from hyaluronan (Fig. 5d). Hyaluronan (Fig. 5d) shows one principal exothermic peak which seems to be, in fact, composed from two peaks. These correspond to degradation shown also on TG record including correspondence in interval of degradation temperatures and indication of two peaks on DTG record. Pure hyaluronan fibers and hyaluronan fibers with silver nanoparticles (Fig. 5e and f) show composite records at lower temperatures

which also corresponding to TG records. First, a small exothermic peak is indicated followed by stronger endothermic response with irregular shape, indicating that it could reflect several processes, which seems to pass to a weak exothermic response. This complex response is not easy to analyze and indicate changes in hyaluronan thermal behavior brought about by fiber making process.

Generally, making fibers significantly changed hyaluronan degradation pattern as detected by DSC. Main hyaluronan degradation peak (exothermic) is almost “removed” and “transformed” to endothermic response (which probably interferes with the exothermic response). This change seems not to be due to the effect of silver nanoparticles but a result of fiber making process. The main endothermic peak could be attributable to:

- some phase transition (but TG shows mass decrease) of structures formed or of impurities entrapped during fiber making process,
- endothermic reaction of these impurities.

Taking into account TG records it seems that to the mass loss corresponds the first, exothermic, part of DSC peaks of pure hyaluronan fibers, and hyaluronan fibers with silver nanoparticles (Fig. 5e and f at about 190 °C) and the following, endothermic, part covers processes detected by TG. Addition of silver nanoparticles has only a minor effect on the onset temperature of thermal degradation but probably influences its mechanism. During the fiber making process some structures are formed undergoing endothermic transformation around 200 °C (together with

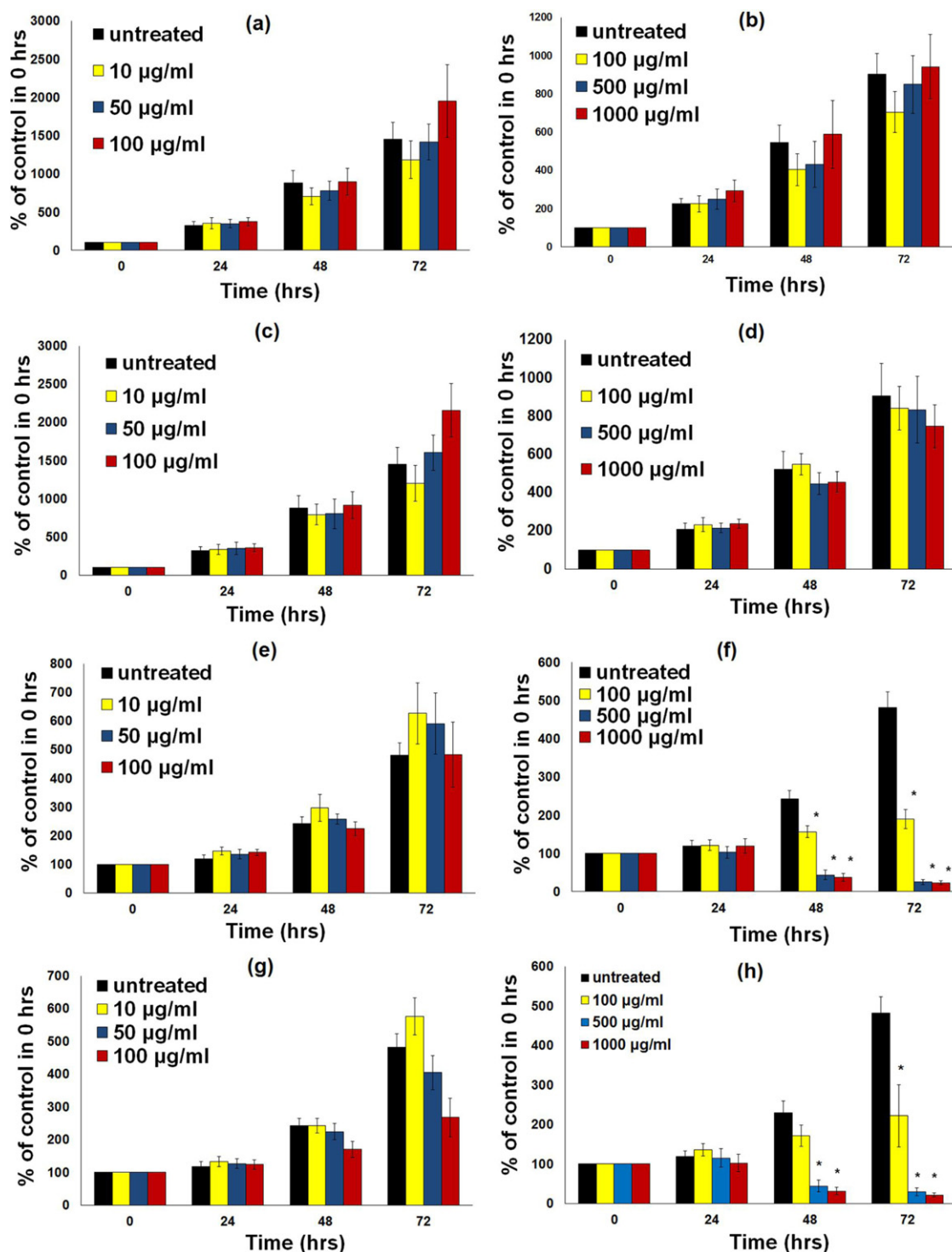


Fig. 7. Effect of hyaluronan, hyaluronan fiber, and hyaluronan fiber with silver nanoparticle (HA-Ag NPs) on cell viability at different time and different concentrations of the components. (a) Hyaluronan concentration (10–100 µg/ml), 3T3 viability, MTT, n = 6; (b) hyaluronan concentration (100–1000 µg/ml), 3T3 viability, MTT, n = 6; (c) hyaluronan fiber concentration (10–100 µg/ml), 3T3 viability, MTT, n = 6; (d) hyaluronan fiber concentration (100–1000 µg/ml), 3T3 viability, MTT, n = 6; (e) HA-Ag NPs with particle size 10 nm (10–100 µg/ml), 3T3 viability, MTT, n = 6; (f) HA-Ag NPs with particle size 10 nm (100–1000 µg/ml), 3T3 viability, MTT, n = 6; (g) HA-Ag NPs with particle size 40 nm (10–100 µg/ml), 3T3 viability, MTT, n = 6; (h) HA-Ag NPs with particle size 40 nm (100–1000 µg/ml), 3T3 viability, MTT, n = 6.

degradation of fibers). These structures could be either formed by rearrangement of hyaluronan chains during the process of the preparation of fiber and silver nanoparticles. Endothermic transformation occurs in the same time as the main degradation of fibers, indicating existence of (at least) two phase system in fibers.

3.6. XPS of hyaluronan fiber with silver nanoparticles

To make clear the encapsulation state of the obtained silver nanoparticles, the XPS technique was employed to detect the composition of the silver nanoparticles (Fig. 6). The binding energy was referenced to the standard C 1s at 284.667 eV. Fig. 6a shows the



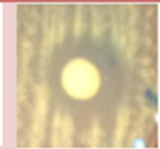
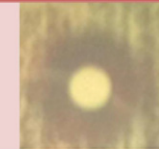
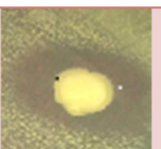
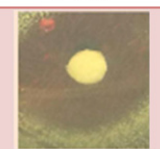
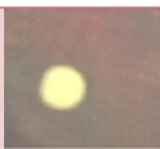
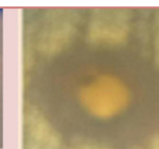

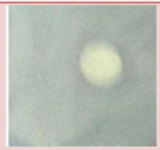

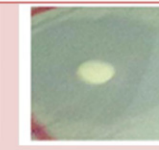
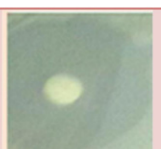

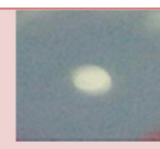

	Control	0.1 mM	0.5 mM	1 mM
E. coli Gram negative				
Particle size (nm)	0	10	12	15
Inhibition zone (mm)	0	5	10	14
	3 mM	5 mM	10 mM	15 mM
E. coli Gram negative				
Particle size (nm)	30	9	10	60
Inhibition zone (mm)	14	25	40	16
	Control	0.1 mM	0.5 mM	1 mM
S. aureus Gram positive				
Particle size (nm)	0	6	12	18
Inhibition zone (mm)	0	4	10	17
	3 mM	5 mM	10 mM	15 mM
S. aureus Gram positive				
Particle size (nm)	20	21	38	20
Inhibition zone (mm)	20	25	28	35

Fig. 8. Comparison of the inhibition zone test between Gram-negative and Gram-positive bacteria (*Escherichia coli* (*E. coli*) and *Staphylococcus aureus* (*S. aureus*)) of hyaluronan fiber-silver nanoparticles (HA-Ag NPs) prepared with different concentrations of silver nitrate and different particles sizes.

XPS survey spectra of the hyaluronan fiber with silver nanoparticles; the atoms of C, N, O, Na and Ag were detected, and no other obvious peaks were found, indicating high purity of the sample. The binding energies at 284.182 eV and 399.66 eV arose from C 1s and N 1s respectively (Fig. 6b and c). The N 1s peak was resolved into two peaks at 399.346 and 398.867 eV respectively. The 398.867 eV peak suggested the presence of charged nitrogen atoms, indicating an electrostatic interaction with the silver surface. The peak at 399.66 eV was assigned to C–N units, which suggested interaction between these N atoms and the silver nanoparticles. From the spectra of Ag 3d (Fig. 6d), the binding energies for Ag 3d_{5/2} and Ag 3d_{3/2} were found to be 367.329 eV and 373.392 eV respectively, which were compared to the respective core levels of bulk Ag crystals (368 and 374 eV) (Sharma, Chaki, Mandale, Pasricha, & Vijayamohan, 2004). Moreover, the narrow width of the peaks suggested that only single-element silver was present in the system, and provided evidence for the encapsulation of zero valence silver nanoparticles by hyaluronan fiber macromolecules. The results of the XPS spectra revealed that hyaluronan fiber could stabilize the silver nanoparticles from aggregation and provided supporting evidence for the hyaluronan fiber-encapsulated silver nanoparticle structure.

3.7. Effect of hyaluronan fiber with silver nanoparticles on the cell viability

Fig. 7 shows the effect of pure hyaluronan (10–1000 µg/ml; Fig. 7a and b), hyaluronan fiber (10–1000 µg/ml; Fig. 7c and d), and hyaluronan fibers with silver nanoparticles with different particle sizes (10–1000 µg/ml; Fig. 7e and f – 10 nm) (Fig. 7g and h – 40 nm) on cell viability of NIH 3T3 cell line. Viability test MTT was utilized to obtain basic information about cell metabolism and proliferation. The MTT assay is based on the reduction of the yellow tetrazolium salt to insoluble purple formazan crystals by metabolically viable cells. MTT test is rapid, versatile, quantitative, high reproducible and it is useful in screening programs. MTT assay provide fundamental safety data required for the following tests.

On the basis of obtained results from cell viability hyaluronan and pure hyaluronan fiber (up to 1000 µg/ml) were not cytotoxic for NIH 3T3 cell line. The viability of cells after their treatment was not significantly changed in whole monitored interval 24–72 h after treatment (Fig. 7a–d).

Effect of the particle size of Ag NPs on the cell viability (Fig. 7e–h), Fig. 7e–h shows the cell viability of hyaluronan fiber with silver nanoparticles particles size approximately 10 and 40 nm measured

by DLS technique. HA-Ag NPs (10 and 40 nm) with concentration from (10–100 $\mu\text{g/ml}$) were nontoxic (Fig. 7e and g), but HA-Ag NPs, where the concentration was up to 100 $\mu\text{g/ml}$, were cytotoxic 48 and 72 h (Fig. 7f and h). These results showed that hyaluronan fiber with silver nanoparticles with different particle sizes 10, 40 nm for a concentration until 100 $\mu\text{g/ml}$ were safety for next biological activity experiments.

3.8. Antibacterial activity of hyaluronan-silver nanoparticles (HA-Ag NPs)

The inhibition zone values were determined for the prepared samples were tested against two types of bacteria, *E. coli*, and *S. aureus* of hyaluronan fiber-silver nanoparticles (HA-Ag NPs). Results and images for the inhibition zones were presented as average values (mm) as shown in Fig. 8. The obtained data demonstrates that all the investigated hyaluronan fiber-silver nanoparticles (HA-Ag NPs) had relatively high and almost similar antibacterial activity against Gram-positive (*S. aureus*) and Gram-negative (*E. coli*) bacteria as compared to that of control. This relatively high antibacterial activity can be attributed to the size and the high surface area of the hyaluronan fiber-silver nanoparticles which enabled them to reach easily the nuclear content of bacteria (Chen, Li, Qian, & Xu, 2010; Chudasama, Vala, & Andhariya, 2009; Jeong, Hwnag, & Yi, 2005; Lee, Cohen, & Rubner, 2005; Lok et al., 2006; Morones, Elechiguerra, & Camacho, 2005; Morones, Elechiguerra, Camacho, Holt, et al., 2005). It is apparent also from the data in Fig. 8 that an increase of the concentration of the hyaluronan fiber-silver nanoparticles was increasing.

The mechanism of the bactericidal effect of silver colloid particles against bacteria is not very well known. It is possible that Ag NPs act similarly to the antimicrobial agents used for the treatment of bacterial infections. Those agents show four different mechanisms of action: (1) interference with cell wall synthesis; (2) inhibition of protein synthesis; (3) interference with nucleic acid synthesis; and (4) inhibition of a metabolic pathway (Tenover, 2006). Three different mechanisms of action of Ag NPs have been proposed by Feng et al. (2000).

First, Ag NPs attach to the surface of the cell membrane and disturb its power functions, such as permeability and respiration (Murray, Steed, & Elson, 1965). Plasmolysis (cytoplasm separated from bacterial cell wall) in *Pseudomonas aeruginosa* and the inhibition of bacterial cell wall synthesis in *S. aureus* bacteria were reported by Song, Ko, and Lee (2006). It is reasonable to state that the binding of the particles to the bacteria depends on the interaction of the surface area available. Smaller particles having a larger surface area available for interaction will have a stronger bactericidal effect than will larger particles (Shrivastava et al., 2007). This is moderately in accordance with the results shown in Fig. 8.

Second, Ag NPs are able to penetrate the bacteria and cause further damage, possibly by interacting with sulfur- and phosphorus-containing compounds such as DNA. Gibbins and Warner (2005) and Raffi et al. (2008) reported TEM images of Ag NPs in the membranes of the bacteria as well as in the interior. In addition, it is believed that Ag NPs after penetration into the bacteria have inactivated their enzymes, generating hydrogen peroxide and causing bacterial cell death (Raffi et al., 2008; Shockman & Barrett, 1983).

In addition, it is believed that the high affinity of silver for sulfur or phosphorus is the key element of its antibacterial property, in that sulfur and phosphorus are found in abundance throughout the cell membrane. Ag NPs react with sulfur containing proteins inside or outside the cell membrane, which in turn affects cell viability (Hamouda & Baker, 2000).

Third, Ag NPs release silver ions, which make an additional contribution to the bactericidal effect (Feng et al., 2000). In

fact, Morones, Elechiguerra, and Camacho (2005) and Morones, Elechiguerra, Camacho, Holt, et al. (2005) showed that Ag NPs (where silver is present in the Ag^0 form) also contain micro molar concentrations of Ag^+ , and they have shown that Ag^+ and Ag^0 both contribute to the antibacterial activity. The mechanism of inhibition by silver ions on microorganisms is partially known. It is believed that DNA loses its replication ability and cellular proteins become inactivated on silver ion treatment (Gupta, Bajpai, & Bajpai, 2008; Kumar, Kumar-Vemula, Ajayan, & John, 2008). Higher concentrations of Ag^+ ions have been shown to interact with cytoplasmic components and nucleic acids (Feng et al., 2000; Kim, 2007a, 2007b).

The antibacterial effect of Ag NPs determined in this study was found to be similar to that described in the earlier reports (Shrivastava et al., 2007), the particle size has an effect on microbes; the effect increased with smaller particle size. In our case we have a distribution of particle sizes with a mean diameter ranging from 10 nm to 60 nm. From the results in Fig. 8 we can say that there is a relationship between the size of the nanoparticles and the bacterial activity. In spite of the strong antibacterial activity of the developed hyaluronan fiber-silver nanoparticles, further studies are required to investigate their bactericidal effects on different types of bacteria for potential widening of their applications especially for medical applications such as wound healing and dressing.

4. Conclusions

Hyaluronan fibers with silver nanoparticles were successfully prepared using green approach and their purity and structure were analyzed by techniques such as UV/Vis spectroscopy, TEM, DLS, TGA, DTG, DSC, FTIR, NMR and XPS. This methodology can also be adapted to the preparation of other metal nanoparticles. Results of silver nanoparticles incorporated in hyaluronan fibers showed high biological activity. Hyaluronan fiber with silver nanoparticles was nontoxic using mouse fibroblast cell line NIH 3T3. Thus, Ag NPs incorporated in the hyaluronan fibers can be used in the different biomedical purposes especially in wound healing and dressing purposes.

References

- Abdel-Mohsen, A. M., Abdel-Rahman, M. R., Hrdina, R., Imramovský, A., Burgert, L., & Aly, A. S. (2012). Antibacterial cotton fabrics treated with core shell nanoparticles. *International Journal of Biological Macromolecules*, 50, 1245–1253.
- Abdel-Mohsen, A. M., Aly, A. S., Hrdina, R., & El-Aref, A. T. (2012). A novel method for the preparation of silver/chitosan-O-methoxy polyethylene glycol core shell nanoparticles. *Journal of Polymers and the Environment*, 20, 459–468.
- Abdel-Mohsen, A. M., Hrdina, R., Burgert, L., Krylova, G., Abdel-Raman, R., Krylova, A., et al. (2012). Green synthesis of hyaluronan fibers with silver nanoparticles. *Carbohydrate Polymers*, 89, 411–422.
- Antonio, S. O., & Andre, L. G. (2010). Laser ablated silver nanoparticles with nearly the same size in different carrier media. *Journal of Nanomaterials*, 5, 1–7.
- Bauer, A. W., Kirby, M. M., Sherris, J. C., & Truck, M. (1966). Antibiotic susceptibility testing by a standardized single disk method. *American Journal of Clinical Pathology*, 45, 493–406.
- Burgert, L., Hrdina, R., Masek, D., & Velebný, V. (2012). *Fibers from hyaluronan, their preparation and application*. CZ 302994 B6 0208. CPN spol. s.r.o. Dolní Dobrouč, Czech Republic.
- Chen, S. F., Li, J. P., Qian, K., & Xu, W. P. (2010). Large scale photochemical synthesis M@TiO_2 nanocomposites (M=Ag, Pd, Au, Pt) and their optical properties, CO oxidation performance and antibacterial effect. *Nano Research*, 3, 244–255.
- Chudasama, B., Vala, A. V., & Andhariya, N. (2009). Enhanced antibacterial activity of bifunctional Fe_3O_4 core-shell nanostructures. *Nano Research*, 2, 955–965.
- Dagalakis, N., Flink, J., Stasikelis, P., Burke, J. F., & Yannas, I. V. (1980). Design of an artificial skin. III. Control of pore structure. *Journal of Biomedical Materials Research Part A*, 14, 511–518.
- Dash, M., Chiellini, F., Ottenbrite, R. M., & Chiellini, E. (2011). Chitosan – A versatile semi-synthetic polymer in biomedical applications. *Progress in Polymer Science*, 26, 981–1014.
- David-Raoudi, M., Tranchepain, F., Deschrevel, B., Vincent, J. C., Bogdanowicz, P., Boumediene, K., et al. (2008). Differential effects of hyaluronan and its fragments

- on fibroblasts: Relation to wound healing. *Wound Repair and Regeneration*, 16, 274–287.
- Difco et al. (1969). Laboratories Incorporated Detroit Michigan, 48201, U.S.A.
- Emilio, I., Alarcon, K., Udekwa, M., Skog, N. L., Pacion, K. G., Stampleskoskie, M., et al. (2012). The biocompatibility and antibacterial properties of collagen-stabilized, photochemically prepared silver nanoparticles. *Biomaterials*, 33, 4947–4956.
- Farooqui, M. A., Chauhan, P. S., Krishnamoorthy, P., & Shaik, J. (2010). Extraction of silver nanoparticles from the leaf extracts of clerodendrum inerme. *Digest Journal of Nanomaterials and Biostructures*, 5, 43–48.
- Feng, Q. L., Wu, J., Chen, G. Q., Cui, F. Z., Kim, T. N., & Kim, J. O. (2000). A mechanistic study of the antibacterial effect of silver ions on *E. coli* and *Staphylococcus aureus*. *Journal of Biomedical Materials Research*, 52, 662–668.
- Gibbins, B., & Warner, L. (2005). The role of antimicrobial silver nanotechnology. *Medical Device & Diagnostic Industry Magazine*, 1, 1–2.
- Gupta, P., Bajpai, M., & Bajpai, S. K. (2008). Investigation of antibacterial properties of silver nanoparticle-loaded poly (acrylamide-co-itaconic acid)-grafted cotton fabric. *Journal of Cotton Science*, 12, 280–286.
- Hamouda, T., & Baker, J. R., Jr. (2000). Antimicrobial mechanism of action of surfactant lipid preparations in enteric gram-negative bacilli. *Journal of Applied Microbiology*, 89, 397–403.
- Jae, Y. S., & Beom, S. K. (2009). Rapid biological synthesis of silver nanoparticle using plant leaf extracts. *Bioprocess and Biosystems Engineering*, 32, 79–84.
- Jeong, S. H., Hwnag, Y. H., & Yi, S. C. (2005). Antibacterial properties of padded PP/PE nonwovens incorporating nano-sized silver colloids. *Journal of Materials Science*, 40, 5413–5418.
- Ji, M., Chen, X., Wai, C. M., & Fulton, J. L. (1999). Synthesizing and dispersing silver nanoparticles in a water-in-supercritical carbon dioxide microemulsion. *Journal of American Chemical Society*, 121, 2631–2632.
- Kim, J. S. (2007a). Antibacterial activity of Ag⁺ ion-containing silver nanoparticles prepared using the alcohol reduction method. *Journal of Industrial and Engineering Chemistry*, 13, 718–722.
- Kim, J. S. (2007b). Reduction of silver nitrate in ethanol by poly(N-vinyl pyrrolidone). *Industrial & Engineering Chemistry Research*, 13(4), 566–570.
- Kumar, A., Kumar-Vemula, P., Ajayan, P. M., & John, G. (2008). Silver-nanoparticle embedded antimicrobial paints based on vegetable oil. *Nature Materials*, 7, 236–241.
- Lee, D., Cohen, R. E., & Rubner, M. F. (2005). Antibacterial properties of Ag nanoparticle loaded multilayers and formation of magnetically directed antibacterium. *Langmuir*, 21, 9651–9659.
- Lees, V. G., Fan, T. P., & West, D. C. (1995). Angiogenesis in a delayed revascularization model is accelerated by angiogenic oligosaccharides of hyaluronan. *Laboratory Investigation*, 73, 259–266.
- Lim, B., Jiang, M., & Yu, T. (2010). Nucleation and growth mechanisms for Pd–Pt bimetallic nano dendrites and their electro catalytic properties. *Nano Research*, 3, 69–80.
- Lin, S. Y., Chen, K. S., & Run, C. L. (2001). Design and evaluation of drug loaded wound dressing having thermo responsive, adhesive, absorptive and easy peeling properties. *Biomaterials*, 22, 2999–3004.
- Lok, C. N., Ho, C. M., Chen, R., He, Q. Y., Yu, W. Y., & Sun, H. (2006). Proteomic analysis of the mode of antibacterial action of silver nanoparticles. *Journal of Proteome Release*, 5, 916–924.
- Luis, M. M., & Isabel, T. (1996). Reduction and stabilization of silver nanoparticles in ethanol by nonionic surfactants. *Langmuir*, 12, 3585–3589.
- Marsano, A., Millward-Sadler, S. J., Salter, D. M., Adesida, A., Hardingham, T., Tognana, E., et al. (2007). Differentia cartilaginous tissue formation by human synovial membrane, fat pad, meniscus cells and articular chondrocytes. *Osteoarthritis and Cartilage*, 15, 48–58.
- Morones, J. R., Elechiguerra, J. L., & Camacho, A. (2005). The bactericidal effect of silver nanoparticles. *Nanotechnology*, 16, 2346–2353.
- Morones, J. R., Elechiguerra, J. L., Camacho, A., Holt, K., Kouri, J. B., & Tapia, J. (2005). The bactericidal effect of silver nanoparticles. *Nanotechnology*, 16, 2346–2353.
- Murray, R. G. E., Steed, P., & Elson, H. E. (1965). The location of the mucopeptide in sections of the cell wall of *Escherichia coli* and other gram-negative bacteria. *Canadian Journal of Microbiology*, 11, 547–560.
- Panacek, A., Kolar, M., Vecerova, R., Pucek, R., Soukupova, J., Krystof, V., et al. (2009). Antifungal activity of silver nanoparticles against *Candida* spp. *Biomaterials*, 30, 6333–6340.
- Pathak, S., Greci, M. T., & Kwong, R. C. (2000). Synthesis and applications of palladium-coated poly(vinyl pyridine) nanospheres. *Chemical Material*, 12, 1985–1989.
- Price, R. D., Berry, M. G., & Navsaria, H. A. (2007). Hyaluronic acid: The scientific and clinical evidence. *Journal of Plastic Reconstructive & Aesthetic Surgery*, 60, 1110–1119.
- Proctor, M., Proctor, K., Shu, X. Z., McGill, L. D., Prestwich, G. D., & Orlandi, R. R. (2006). Composition of hyaluronan affects wound healing in the rabbit maxillary sinus. *American Journal of Rhinology & Allergy*, 20, 206–211.
- Purna, S. K., & Babu, M. (2000). Collagen based dressings – A review. *Burns*, 26, 54–62.
- Raffi, M., Hussain, F., Bhatti, T. M., Akhter, J. I., Hameed, A., & Hasan, M. M. (2008). Antibacterial characterization of silver nanoparticles against *E. coli* ATCC-15224. *Journal of Materials Science & Technology*, 24, 192–196.
- Rajapaksa, S. P., Cowin, A., Adams, D., & Wormald, P. J. (2005). The effect of a hyaluronic acid based nasal pack on mucosal healing in a sheep model of sinusitis. *American Journal of Rhinology & Allergy*, 19, 572–576.
- Raveendran, P., Fu, J., & Wallen, S. L. (2003). Completely green synthesis and stabilization of metal nanoparticles. *American Chemical Society*, 125, 13940–13941.
- Raveendran, P., Fu, J., & Wallen, S. L. (2006). A simple and green method for the synthesis of Au, Ag, and Au–Ag alloy nanoparticles. *Green Chemistry*, 8, 34–38.
- Robert, P., Tucek, J., Kilianová, M., Panáček, A., Kvíte, L., Filip, J., et al. (2011). The targeted antibacterial and anti-fungal properties of magnetic nanocomposite of iron oxide and silver nanoparticles. *Biomaterials*, 32, 4704–4713.
- Rooney, P., Wang, M., Kumar, P., & Kumar, S. (1993). Angiogenic oligosaccharides of hyaluronan enhance the production of collagen by endothelial cells. *Journal of Cell Science*, 105, 213–218.
- Schimizzi, A. L., Massie, J. B., Murphy, M., Perry, A., Kim, C. W., Garfin, S. R., et al. (2006). High-molecular-weight hyaluronan inhibits macrophage proliferation and cytokine release in the early wound of a preclinical postlaminectomy rat model. *The Spine Journal*, 6, 550–556.
- Shah, P. S., Holmes, J. D., Doty, R. C., Johnston, K. P., & Korgel, B. A. (2000). Steric stabilization of nanocrystals in supercritical CO₂ using fluorinated ligands. *Journal of American Chemical Society*, 122, 4245–4246.
- Shameli, K., Ahmad, M. B., & Yunus, W. (2010). Silver/poly(lactic acid) nanocomposites, preparation, characterization, and antibacterial activity. *International Journal of Nanomedicine*, 5, 573–579.
- Sharma, J., Chaki, N. K., Mandale, A. B., Pasricha, R., & Vijayamohan, K. (2004). Controlled interlinking of Au and Ag nanoclusters using 4-aminothiophenol as molecular interconnects. *Journal of Colloid and Interface Science*, 272, 145–152.
- Shen, J., Shi, M., & Li, N. (2010). Facile synthesis and application of Ag-chemical converted graphene nanocomposites. *Nano Research*, 3, 339–349.
- Shockman, G. D., & Barrett, J. F. (1983). Structure, function, and assembly of cell walls of gram-positive bacteria. *Annual Review of Microbiology*, 37, 501–527.
- Shrivastava, S., Bera, T., Roy, A., Singh, G., Ramachandrarao, P., & Dash, D. (2007). Characterization of enhanced antibacterial effects of novel silver nanoparticles. *Nanotechnology*, 18(22), 5103–5112.
- Singh, A., Jain, D., Upadhyay, M. K., Khandelwal, N., & Verma, H. N. (2010). Green synthesis of silver nanoparticles using agrimony Mexicana leaf extract and evaluation of their antimicrobial activities. *Digest Journal of Nanomaterials and Biostructures*, 5, 659–665.
- Slevin, M., Krupinski, J., Gaffney, J., Matou, S., West, D., Delisser, H., et al. (2007). Hyaluronan-mediated angiogenesis in vascular disease: Uncovering RHAMM and CD44 receptor signaling pathways. *Matrix Biology*, 26, 58–68.
- Slevin, M., Kumar, S., & Gaffney, J. (2002). Angiogenic oligosaccharides of hyaluronan induce multiple signaling pathways affecting vascular endothelial cell mitogen and wound healing responses. *Journal of Biological Chemistry*, 277, 41046–41059.
- Smith, M. M., Cake, M. A., Ghosh, P., Schiavinato, A., Read, R. A., & Little, C. B. (2008). Significant synovial pathology in a meniscectomy model of osteoarthritis: Modification by intra-articular hyaluronan therapy. *Journal of Rheumatology*, 47, 1172–1178.
- Song, H. Y., Ko, K. K., & Lee, B. T. (2006). Fabrication of silver nanoparticles and their antimicrobial mechanisms. *European Cells & Materials*, 11, 58–59.
- Takahashi, Y., Li, L., Kamiryo, M., Asteriou, T., Moustakas, A., Yamashita, H., et al. (2005). Hyaluronan fragments induce endothelial cell differentiation in a CD44- and CXCL1/GRO1-dependent manner. *Journal of Biological Chemistry*, 280, 24195–24204.
- Templeton, A. C., Chen, S., Cross, S. M., & Murray, R. W. (1999). Water-soluble, isolable gold clusters protected by tiopronin and coenzyme A monolayers. *Langmuir*, 15, 66–76.
- Tenover, F. C. (2006). Mechanisms of antimicrobial resistance in bacteria. *American Journal of Medicine*, 119, 3–10.
- Tezel, A., & Fredrickson, G. H. (2008). The science of hyaluronic acid dermal fillers. *Journal of Cosmetic and Laser Therapy*, 10, 35–42.
- Uppendra, K. P., Preeti, S. S., & Anchal, S. (2009). Bioinspired synthesis of silver nanoparticles. *Digest Journal of Nanomaterials and Biostructures*, 4, 159–166.
- Vigneshwaran, N., Nachane, R. P., Balasubramanya, R. H., & Varadarajan, P. V. (2006). A novel one-pot green synthesis of stable silver nanoparticles using soluble starch. *Carbohydrate Research*, 341, 2012–2018.
- Vistejnova, L., Dvorakova, J., Hasova, M., Muthny, T., Velebný, V., Soucek, K., et al. (2009). The comparison of impedance-based method of cell proliferation monitoring with commonly used metabolic-based techniques. *Neuroendocrinology Letters*, 1(121), 127.
- Wan, A., Sun, Y., Li, G., & Li, H. L. (2009). Preparation of aspirin and probucol in combination loaded chitosan nanoparticles and in vitro release study. *Carbohydrate Polymers*, 75, 566–574.
- Wang, Y., Ren, J., & Deng, K. (2000). Preparation of tractable platinum, rhodium, and ruthenium nanoclusters with small particle size in organic media. *Chemical Material*, 12, 1622–1627.
- West, D. C., Hampson, I. N., Arnold, F., & Kumar, S. (1985). Angiogenesis induced by degradation products of hyaluronic acid. *Science*, 228, 1324–1326.